PLOS ONE

Prevention of Transfusion-Associated Graft-versus-Host Disease by Irradiation: Technical Aspect of a New Ferrous Sulphate Dosimetric System

Lucas Sacchini Del Lama[1]*, Evamberto Garcia de Góes[2], Paulo César Dias Petchevist[1], Edson Lara Moretto[3], José Carlos Borges[3], Dimas Tadeu Covas[3,4], Adelaide de Almeida[1]

1 Physics Department, School of Philosophy, Sciences and Letters of Ribeirão Preto, University of São Paulo (FFCLRP/USP), Ribeirão Preto, São Paulo, Brazil, 2 Mathematics, Statistics and Physics Institute, Federal University of Rio Grande (IMEF/FURG), Rio Grande, Rio Grande do Sul, Brazil, 3 Regional Blood Center of Ribeirão Preto, Ribeirão Preto, São Paulo, Brazil, 4 Center for Cell-Based Therapy, School of Medicine of Ribeirão Preto, University of São Paulo, Ribeirão Preto, São Paulo, Brazil

Abstract

Irradiation of whole blood and blood components before transfusion is currently the only accepted method to prevent Transfusion-Associated Graft-Versus-Host-Disease (TA-GVHD). However, choosing the appropriate technique to determine the dosimetric parameters associated with blood irradiation remains an issue. We propose a dosimetric system based on the standard Fricke Xylenol Gel (FXG) dosimeter and an appropriate phantom. The modified dosimeter was previously calibrated using a ^{60}Co teletherapy unit and its validation was accomplished with a ^{137}Cs blood irradiator. An ionization chamber, standard FXG, radiochromic film and thermoluminescent dosimeters (TLDs) were used as reference dosimeters to determine the dose response and dose rate of the ^{60}Co unit. The dose distributions in a blood irradiator were determined with the modified FXG, the radiochromic film, and measurements by TLD dosimeters. A linear response for absorbed doses up to 54 Gy was obtained with our system. Additionally, the dose rate uncertainties carried out with gel dosimetry were lower than 5% and differences lower than 4% were noted when the absorbed dose responses were compared with ionization chamber, film and TLDs.

Introduction

Transfusion-Associated Graft-Versus-Host Disease (TA-GVHD) is a rare, but fatal potential complication that occurs when viable donor T lymphocytes proliferate and engraft in susceptible patients after transfusion [1–3]. At least three factors appear to be directly related to the risk of TA-GVHD [4]: 1) the susceptibility of the patient immune system to the engraftment, 2) the degree of Human Leukocyte Antigen (HLA) similarity between donor and recipient and 3) the number and viability of donor T lymphocytes present in the transfused components.

According to the literature, cases of TA-GVHD have been reported in severely immunocompromised patients, including patients with congenital immunodeficiencies, in bone marrow transplant recipients, as well as in cancer patients treated with chemotherapy or radiotherapy [2,5–15]. This serious transfusion associated adverse reaction has also been reported in presumed immunocompetent patients who received blood from homozygous donors with shared HLA haplotypes or from a family member [16–35].

Although the minimum concentration of lymphocytes in the donor blood that can initiate TA-GVHD is unknown, a number of lymphocytes as low as 1×10^4/kg of the recipient weight may be sufficient to cause TA-GVHD [36]. The referred report corroborates with other works and indicates that even leukocyte-depleted blood products can promote this reaction [37,38]. Because there is no effective treatment for TA-GVHD [39,40], irradiation of whole blood and blood components prior to transfusion is the only proven method to prevent the reaction [41,42]. Ionizing radiation breaks the DNA molecules of T lymphocytes and prevents an immune response against the recipient [3,43,44].

Blood irradiation can be performed using commercial irradiators specifically designed for this purpose, which are usually located in blood banks. These dedicated blood irradiators use radioactive isotopes such as ^{137}Cs or ^{60}Co, which emit gamma-rays, or linear accelerators, which emit X-rays. Based on previous data about the elimination of allogeneic reactivity using Mixed Lymphocyte Culture analysis (MLC), at least 15 Gy was recommended for irradiation of blood components [45,46]. However, at least three cases of TA-GVHD were reported in patients who received blood irradiated with doses between 15 and 20 Gy [47–49]. More recently, studies on the radiosensitivity of T-cells to gamma and X-rays, assessed by Limiting Dilution Analysis (LDA), have shown that an absorbed dose of 25 Gy is necessary to prevent TA-GVHD [28,44,50]. Under this exposure condition, damages are minimal to granulocytes and anucleate cells as

erythrocytes (RBCs) and platelets (PLTs). Thus, Food and Drug Administration (FDA) [51] and the American Association of Blood Banks (AABB) [52] specify a dose of 25 Gy at the middle plane of the blood component. Similarly, the European and the British guidelines state that a minimum dose should be 25 Gy and no more than 50 Gy for each blood bag [53–56]. In order to meet these requirements, a dosimetric system must determine 1) the dose rate and the dose in the blood bags and 2) the spatial dose distribution in the irradiated blood volume.

A Fricke dosimeter is a chemical dosimeter, first proposed in 1927 by Hugo Fricke and Sterne Morse [57] as an acidic oxygenated ferrous sulphate solution. The absorbed dose is inferred through the radiation induced oxidation process, in which ferrous ions (Fe^{+2}) oxidize to ferric ones (Fe^{+3}) due to water decomposition [58,59]. This dosimeter has been recommended by the American Association of Physicists in Medicine (AAPM) [60] and the International Commission on Radiation Units and Measurements (ICRU) [61] as an alternative clinical dosimeter owing to its water-equivalent radiological characteristics and achievable absoluteness.

At the end of the last century, many researchers proposed tissue-equivalent dosimeters based on the original Fricke liquid solution, some with gelatin and polymeric matrices instead of liquid. Gelatin dosimetry has been studied since 1950's [62,63], when the gel molecular proprieties began to be studied after ionizing radiation exposures. Some of these gelatins were used to prepare Fricke gel dosimeters, becoming the first dosimetric system able to three-dimensionally map the absorbed dose in a non-destructive and non-invasive manner [64–66]. In fact, one of the most common recipes to prepare this type of dosimeter adds porcine skin gelatin and Xylenol Orange dye to the original solution. This dosimeter is known as Fricke Xylenol Gel (FXG) and was proposed by Gillboy et al in 2000 [67]. The FXG has a linear absorbance response for doses from 0 up to $30-40$ Gy. It has advantages over the liquid solution when spatial resolution and natural oxidation stability are crucial. In addition, the FXG dosimeter allows quantitative and qualitative analysis of the absorbed dose spatial distribution over an irradiated volume [68,69] with various analysis techniques, including UV/visible spectroscopy [67,70–75], magnetic resonance [64–66,71,76–80], Charge-Coupled Device (CCD) [69,81–90] and photoacoustics [91,92].

Because the standard FXG optical response saturates for absorbed doses higher than $30-40$ Gy, we have developed a modified recipe for the FXG dosimeter, which includes lowering the pH, increasing the metal dye concentration and adding sodium chloride to the solution. These modifications provide linear responses for doses up to 50 Gy, as recommended by the blood irradiation guidelines.

Materials and Methods

Irradiation Sources and Calibration

In this study, the standard FXG [67], TLDs (LiF-100, Harshaw Chemical Co., Ohio, USA), radiochromic film (Gafchromic-EBT2, International Specialty Products, New Jersey, USA) and the modified FXG dosimeter were irradiated using one sealed ^{60}Co source (effective energy of 1.25 MeV) from a cobalt teletherapy unit (Theratron-780C, MDS Nordion, Ontario, Canada). Calibration of the ^{60}Co source was accomplished with a calibrated clinical ionization chamber (Farmer-N30001, PTW, Freiburg, Germany) and an electrometer (K35617EBS, Keithley Instruments Inc., Ohio, USA), in accordance with the International Atomic Energy Agency (IAEA) protocol recommendations [93]. Also following this protocol, the standard FXG, TLDs and

film were calibrated in terms of absorbed dose in water and their responses were compared with those obtained with the modified FXG dosimeter. In this sense, the standard FXG, TLDs and film were employed as reference dosimeters to validate the modified FXG response for dosimetry of a gamma blood irradiator (Gammacell® 3000, Best Theratronics Ltd., Ontario, Canada). This irradiator contained one sealed ^{137}Cs source (effective energy of 0.662 MeV) with nominal activity of 53.7 TBq (1,450 Ci), inside of a steel-encased lead shield, able to deliver up to 5.0 Gy per minute at the canister central plane, for default rotation rates (approximately 30 cycles per minute). The blood irradiator dosimetry setup consisted of two different radiation phantoms proposed here.

Since blood and blood components are usually chilled or frozen, standard and modified FXG dosimeters were used for different irradiation temperatures, employing the ^{60}Co teletherapy unit and a water phantom, maintained at the desired temperature (3 and $23\pm1°C$ were evaluated). FXG samples were located inside $1.0\times1.0\times4.5$ cm³ acrylic cuvettes (Plastibrand™, Sigma-Aldrich, Missouri, USA), which were positioned 0.5 cm under the water surface, in accordance with IAEA build-up procedures [93]. The dosimeters were isolated from water by a thin PVC plastic film, in order to avoid possible contamination.

FXG Dosimeter System

The modified FXG recipe was prepared considering 124.38 mM of porcine skin gelatin (270 Bloom, Gelnex, Santa Catarina, Brazil), 0.63 mM of ferrous ammonium sulphate hexahydrate (Merck, Darmstadt, Germany), 0.20 mM of Xylenol Orange, XO, (Merck, Darmstadt, Germany), 48.78 mM of sulphuric acid (J.T. Baker, New Jersey, USA), 0.63 mM of sodium chloride (Sigma-Aldrich, Missouri, USA) and Milli-Q water (Millipore, Massachusetts, USA). Owing to its convenient melting point (40°C, approximately) and visible light transparency, porcine skin gelatin was chosen as the matrix gel. Ferrous ammonium sulphate is the crucial component of the FXG dosimeter because its oxidation (transformation from Fe^{+2} ions to Fe^{+3} ones) is proportional to the absorbed dose in the irradiated dosimeter. These chemical changes produce a visible light spectral band due to XO, a metal ion salt indicator, which bonds only to the Fe^{+3} ions. The FXG induced absorbance after a radiation exposure allows the use of optical techniques, such as spectrophotometry and the CCD system described here. In order to prevent immediate aggregation between XO and naturally oxidized Fe^{+3} ions, sulphuric acid is necessary to reduce the solution pH. Sodium chloride was added to the modified solution to minimize influences from organic impurities and to increase the system reproducibility.

In this research, we studied solutions with pH between 1.0 and 2.5 and XO concentrations between 0.05 and 0.25 mM, in order to reach an adequate FXG recipe for blood irradiation, which is stated hereafter. Considering the modified FXG dosimeter and 100.0 ml of Milli-Q water, dissolve 5.0058 g of gelatin and 0.0037 g of sodium chloride in 75.0 ml of water. Heat the mixture up to 45°C and continuously stir until a clear solution is obtained. Then, dissolve 0.0152 g of XO in 26.0 ml of sulphuric acid and add 12.5 ml of water to this solution. Finally, dissolve 0.0196 g of ferrous ammonium sulphate hexahydrate in the remaining 12.5 ml of water and add the last two solutions to the warm gelatin one. After thorough mixing, fill the appropriate cuvettes for the desired application and cool to obtain a consistent gelatin.

Analysis depends on the fact that, after ionizing radiation exposure, the XO molecules bond 1:1 with Fe^{+3} ions, which result in dyed regions with Optical Densities (ODs) directly proportional to the absorbed dose at every point in the volume. The pre- and

post-irradiation images were registered with a CCD image system using a 24 mm focal length, a f/18 aperture and a shutter speed of 1/100 [86–90]. Later, both images were superimposed and the *OD* variations were processed by a MATLAB® (MathWorks, Massachusetts, USA) computational routine, considering the red and green channels for the modified FXG and film, respectively. We used the following expression:

$$OD(x,y) = log\left[\frac{I_0(x,y)}{I(x,y)}\right], \qquad (1)$$

where *OD(x,y)* is the optical density of the pixel at (x, y), i.e., the *OD* of the xth line crossing the yth column of the acquired image. The quantities $I_0 (x,y)$ and $I(x,y)$ are the color levels of the (x^{th}, y^{th}) pixel corresponding to the pre- and post-irradiation samples, respectively. Thereby, it was possible to establish a relationship between the absorbed dose and the generated *OD* for any radiochromic dosimeters, such as FXG and film. Additionally, a spectrophotometer (Ultrospec^{TM} 6300, General Electric Co., Buckinghamshire, England) was used to compare the absorbance responses between the standard and the modified FXG dosimeters, selecting the 585 nm spectral band and computing the quantity:

$$\Delta A = A - A_0, \qquad (2)$$

in which ΔA is the absorbance difference between irradiated, A, and non-irradiated, A0, samples.

Dosimetry of the Blood Irradiator

Two-dimensional maps, i.e., the absorbed dose spatial distributions, were determined considering a completely filled canister with blood phantoms composed of water or appropriate plastic materials, such as polystyrene or acrylic [41,45,94]. The dosimeters and their corresponding phantoms were positioned inside the blood irradiator canister and irradiated for 1.0 minute. Analysis used the mirrored middle plane dose distributions of the canister, which were plotted as isodose curves.

A dedicated FXG phantom was constructed for the blood irradiator dosimetry. In this phantom, the FXG dosimeter was placed in a cubic cuvette ($12.4 \times 19.4 \times 1.0$ cm^3), surrounded by two semi-cylindrical cuvettes filled with water, as shown in Figures 1A and B. These cuvettes were manufactured with 2.0 mm-thick walls for adequate ^{137}Cs build-up purposes [95]. The phantom geometry was chosen to match that of the canister and simultaneously allow acquisition of the absorbed dose distributions in the central middle plane of the volume.

The same acrylic phantom employed with the FXG dosimeter (Figure 1) was used to perform the blood irradiator dosimetry with film. Thus, a 12.4×19.4 cm^2 film sheet was inserted between the cubic and one of the semi-cylindrical water filled cuvettes. Film determined absorbed dose distributions were evaluated considering the same parameters as those applied for FXG dosimetry, i.e., absorbed doses were determined by the Optical Density method described earlier and mirrored isodose curves were used to represent dose distributions at the central middle plane of the phantom.

A cylindrical homogeneous clear polystyrene phantom was also manufactured, with size and shape matching those of the canister, to measure absorbed doses with TLDs. Clear polystyrene plaques were cut in accordance with the canister dimensions and attached face to face with screws of the same material. Absorbed doses along the central plane of the phantom were measured using three TLDs per cavity, diametrically distributed along some plates
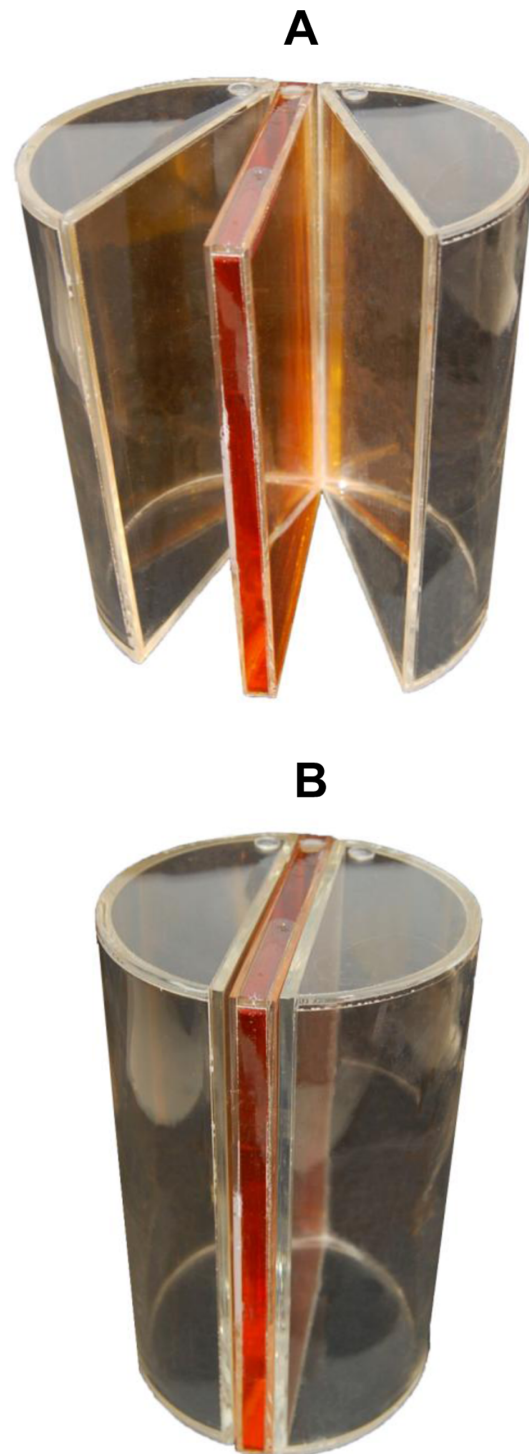
Figure 1. The FXG dosimetric phantom assembly used in the blood irradiator. (A) shows a central cubic dosimeter cuvette filled with the dosimeter and surrounded by two semi-cylindrical water phantoms. (B) shows the mounted FXG phantom.
doi:10.1371/journal.pone.0065334.g001

(Figure 2). After aligning the plates, the TLD-loaded phantom was positioned inside the blood irradiator canister and then irradiated for 1.0 minute. TLDs were previously annealed according to the manufacturer recommendations, i.e., 1 h at 400°C followed by 2 h at 100°C. Dose readings were obtained with a Harshaw reader

Figure 2. Clear polystyrene phantom employed in blood irradiation thermoluminescence dosimetry (TLD). Arrows show some cavities where TLD dosimeters were allocated.
doi:10.1371/journal.pone.0065334.g002

(2000-B/2000-C, Thermo Fisher Scientific Inc., Massachusetts, USA) and a cubic spline interpolation technique was used to represent dose distribution along the central plane of the phantom.

Statistical Analysis

In our study, we considered ten replicated batches for each delivered dose, which ranged from 0 up to 54 Gy. In order to represent the results obtained here, statistical analyses were performed considering averages and standard deviations. The combined standard uncertainty was calculated according to the method stated in the Guide to the Expression of Uncertainty in Measurements [96] and in the ISO/EASTM Estimating Uncertainty in Dosimetry for Radiation Processing [97].

Results

Calibration

Dosimetry of the ^{60}Co beam was performed inside a water tank with an ionization chamber using a 10×10 cm^2 field size, at 80 cm source-to-dosimeter surface distance [93]. The ionization chamber yielded a dose rate of 0.95 Gy per minute, with an uncertainty of less than 3%. For the same irradiation setup, the dose rate measurements were 0.94 Gy per minute with TLD, 0.93 Gy per minute with film and 0.91 Gy per minute with the standard FXG, all uncertainties lower than 5%. The dose rate measured with our modified FXG was 0.97 Gy per minute, with an uncertainty of 4%.

Dose Response and Relative Sensitivity of the Modified FXG Dosimeter

In a dark and temperature controlled ($5 \pm 1^{\circ}$C) environment, absorbances were found to fade exponentially with time after irradiation for the standard FXG, while the modified dosimeter showed no significant fading effects in the first 24 h (Figure 3). After the first day of irradiation, the modified FXG dosimeter showed a smooth linear fading, which persisted during five days of storage.

Figure 4A presents the standard and the modified FXG determined absorbed doses up to 54 Gy, using a spectrophotometer to select the 585 nm absorbance band. The standard dosimeter saturated for doses higher than 40 Gy, while our modified FXG was linear through the full dose range, with linear correlation coefficient (r^2) better than 0.995. An absorbed dose resolution of 0.2 Gy was attained with this setup. Figure 4B presents the *OD* responses for the CCD optical-based technique, compared with those measured by the spectrophotometer. The results are in agreement with those acquired by the previous technique, i.e., the standard FXG dosimeter saturates for higher absorbed doses, while the modified one is linear over the whole range (r$^2 = 0.997$). For this analysis technique, a maximum absorbed dose resolution of 0.5 Gy was attained.

The standard FXG dosimeter showed a sensitivity variation of $0.13 \pm 0.01\%$ per $^{\circ}$C for the spectrophotometric data and of $0.21 \pm 0.02\%$ per $^{\circ}$C for the CCD measurements. In contrast, for the same temperature range, we observed no significant dependencies for the modified FXG dosimeter.

Dosimetry of the Blood Irradiator Unit

The modified FXG and the film dosimeters were used in combination with the water phantoms (Figure 1) and measured by the *OD* method, while TLDs were used in combination with the clear polystyrene phantom (Figure 2) and measured by the Harshaw reader. The ^{137}Cs blood irradiator central dose rates measured with the modified FXG, film and TLDs dosimeters
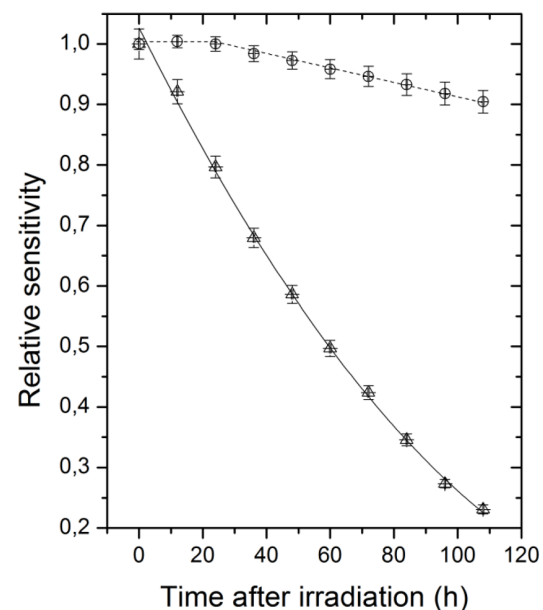

Figure 3. Relative sensitivities for the standard (△) and for the modified (○) FXG dosimeters *versus* time after irradiation. Irradiations were performed considering a known ^{60}Co therapy field.
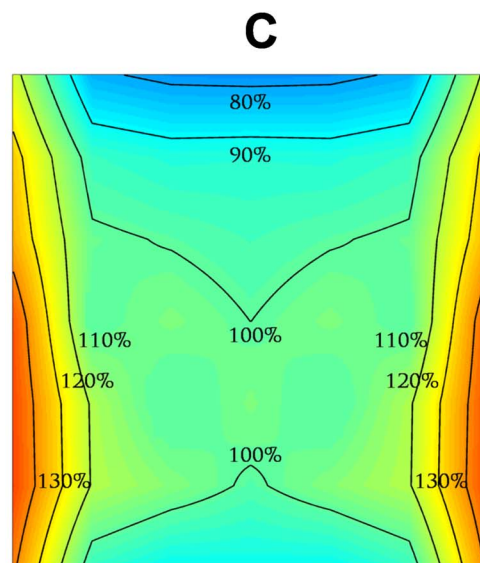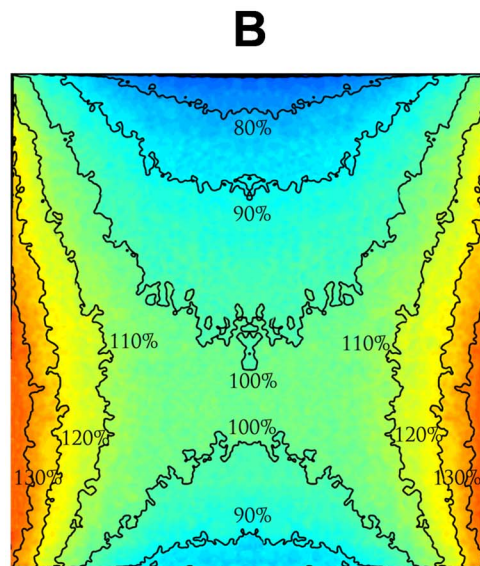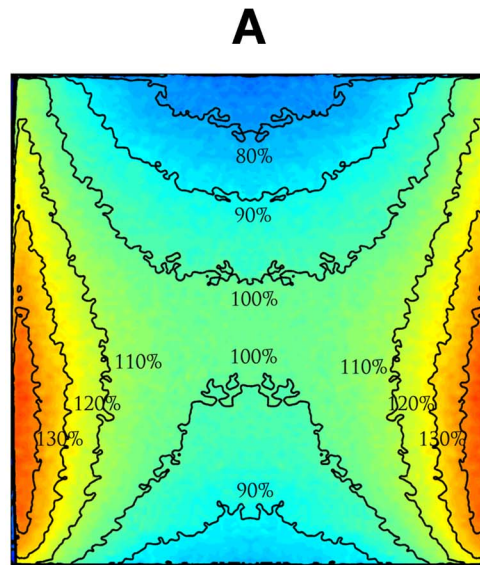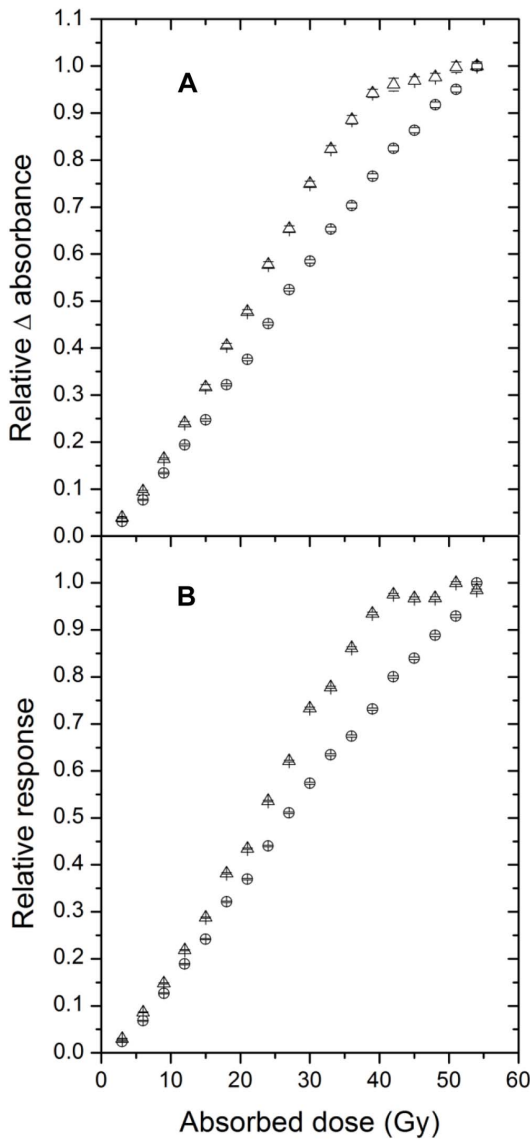doi:10.1371/journal.pone.0065334.g003

Figure 4. Calibration curves obtained for the standard (Δ) and the modified (◦) FXG dosimeters. (A) presents the spectrophotometer absorbance variations, while (B) presents the CCD ODs.
doi:10.1371/journal.pone.0065334.g004

resulted in 5.41, 5.49, and 5.41 Gy per minute, respectively. The dose rate uncertainties associated with TLD and film dosimeters were lower than 3.5%, while the modified FXG dosimeter presented an uncertainty lower than 4.5%.

Figure 5 presents the dose distributions at the central middle plane of the phantoms, in 10% step isodose curves and a color scale. The modified FXG (Figure 5A), the film (Figure 5B) and the TLDs (Figure 5C), show absorbed doses ranging from 74.2±3.7% up to 138.3±4.4%, from 73.6±1.1% to 139.3±1.4% and from 77.7±0.9% to 137.9±2.8%, respectively.

Discussion

Ionization chambers present high accuracy (<3%) and are employed as reference dosimeters by many protocols [60,93,98,99]. For this reason, we used an ionization chamber as a reference dosimeter to calibrate the modified FXG dosimeter proposed here. According to the literature, film and LiF-100

Figure 5. Isodose curves inferred at the canister central plane.
Irradiations were performed at the blood irradiator considering (A) the modified FXG,(B) the film and (C) the TLD dosimeters.
doi:10.1371/journal.pone.0065334.g005

dosimeters also present appropriate features for dosimetric purposes [100–103]. For these reasons, we also selected these dosimeters to validate the modified FXG dosimeter when the blood irradiator was used. Although the standard FXG can also be used for this purpose, saturation effects for doses higher than 40 Gy are the main limitations for its use for blood irradiation. As seen in the calibration results, the dose and dose rate values obtained by the modified FXG dosimeter and those obtained by the ionization chamber were not significantly different. In the same manner, the dose rate associated with the ^{137}Cs blood irradiator determined by the modified FXG dosimeter was not significantly different than those obtained by the standard FXG, film and TLD dosimeters.

FXG is a spectrophotometrically feasible gel matrix [67], which allows optical-based techniques to be applied for data acquisition. Beyond that, the FXG dosimeter response presents low dependence for energies up to 1.25 MeV [104], which avoids the correction factors necessary when this dependence is not negligible. Additionally, the porcine skin gelatin preserves the spatial absorbed dose distribution integrity of the irradiated sample and reduces ions diffusion after exposure. Furthermore, this gelatin is chosen as the gelling agent because it helps to maintain a low FXG effective atomic number (3.35 at 1 MeV) [105] and an adequate mass density (1.05 g per cm^3), which are similar to those of whole blood (3.45 and 1.06 g per cm^3, respectively) [106,107]. Lastly, this gelatin also provides two important features, a reasonable melting point (40°C, approximately), which facilitates preparation, and lower costs than other polymers. For all these reasons, we have developed this dosimeter to optimize its sensitivity, stability and linearity in dose response over the entire dose range used in blood irradiation, besides proposing an appropriate phantom for dosimetric measurements.

According to our findings, we observed a well stabilized relation between the FXG dose response and its pH (non-published data). The pH controls the chemical equilibrium of water radiolysis and consequently the rate associated with the production of free radicals. A higher pH value (>2.0), i.e., more alkaline solution, promotes premature Fe^{+2} oxidation, which leads to early saturations of the FXG response ($\approx$30−40 Gy) and reduction on its linearity (r^2<0.985). In contrast, a lower pH (<1.8) seems to decrease the free radicals production rate and to increase the linear dose response range. This feature is desirable since it allows determination of doses as high as 50 Gy, currently recommended by the guidelines [51–56]. This low pH range also results in higher values of linear correlation factors associated to the FXG response (r^2>0.995), which allows one to acquire information from the response-curve in an effortless way. However, for very low pH values (<1.3), XO−Fe^{+3} can dissociate and data related to dose may be lost. Porcine gelatin structure appeared not to be affected by the pH values investigated (1.0 up to 2.5).

Another important issue concerning the FXG dosimeter is the relation between the solution acidity and its sensitivity. Considering the pH range used here, we observed that the sensitivity associated with the solution was maintained constant ($\approx$0.070 Gy^{-1}cm^{-1}) for pH values higher than 2.0, while it decreased when the pH was reduced. Due to oxygen atoms dissolved in the FXG solution, ferrous ions, Fe^{+2}, are naturally oxidized into ferric ones, Fe^{+3}, which diffuse through the solution. Both effects can be reduced when the solution pH is lowered,

although they continue to occur with time. We observed that a pH value of 1.6 presents reduced natural oxidation and diffusion effects. For these reasons, we propose a FXG recipe with a pH value of 1.6.

We noted that higher Xylenol Orange concentrations yielded wide linear dose ranges and decreased diffusion effects. As stated earlier, XO bond to Fe^{+3} ions in a 1:1 ratio. Although the standard FXG recipe presents a ferrous concentration able to provide responses for doses as high as 100 Gy, its XO concentration does not obey the referred ratio. In fact, similar to the dosimeter pH, the standard XO concentration also contributes to the FXG saturation effects for doses at 30−40 Gy. For a 0.20 mM XO concentration, we obtained adequate linearity for doses up to 54 Gy and reported no significant sensitivity dependence. In this sense, considering the FXG optical response and its corresponding linearity, we propose a FXG recipe with a XO concentration of 0.20 mM.

Sodium chloride aims to control the radiolysis chain reaction, which is initiated in the solution by ionizing radiation. This occurs since Cl atoms prefer to oxidize ferrous ions rather than producing peroxides that accelerate the radiolysis process. We observed better FXG repeatability responses (<3.5%) for a 0.63 mM sodium chloride concentration and lower fading effects when compared to the standard FXG dosimeter. Adequate repeatability and fading are important features for any dosimetric instrument that is intended to provide reliable measurements in a quality control program.

According to our study, the standard FXG response showed a dependence on temperature of 0.13±0.01% per °C, for 3 up to 23±1°C, in agreement (<8%) with results available in literature [108–110]. On the other hand, dependence on temperature showed by the modified FXG dosimeter was not significant. Therefore, the modified FXG is a preferred dosimeter when longer times, such as those for teletherapy blood irradiations (>30 min), are required.

Usually, FXG samples are analyzed at 585 nm in a spectrophotometer. In this study, we used a CCD system in order to better investigate the proprieties related to the FXG dosimeter. The CCD system used in this study allowed us to use three different primary reading channels, namely Red (R), Green (G) and Blue (B). We observed that the red and the green channels presented optimum readings for the FXG and film dosimeters, respectively, when linearity was considered, allied with acceptable sensitivity responses. According to the results obtained here, the CCD resolution in dose was almost 50% lower than that of the spectrophotometer one. However, the linearity responses for both techniques were similar (r^2 = 0.995 for the spectrophotometer and r^2 = 0.997 for the CCD system). While the spectrophotometer is recommended when a higher accuracy in dose is desirable, the CCD system provided adequate linear responses for the FXG dosimeters, as well as high spatial resolutions (<0.5 mm) [90], being completely acceptable for blood dosimetry purposes.

Although blood irradiation has been suggested since 1970s [111] and associated quality control for blood products is well established among different agencies [51–53,55,56], limited attention has been given to the dosimetric aspects of this practice. Qualitatively, there are blood irradiation indicators, used routinely, which only state whether or not the blood bag was irradiated. Different quantitative dosimetric tools have been studied for blood dosimetry in recent years: thermoluminescent dosimetry (TLD) [94,112,113], Fricke solution [112], radiochromic film [114], colorimetric dosimetry [115] and solid state dosimetry, including methacrylate polymers (*red perspex*) [94], alanine [94,116–118], mosfet [41] and diodes [119]. A quantitative method is

commercially available for blood irradiators dosimetry (DOSE-MAP™/Ashland Inc., Covington, Kentucky, USA). However, data need to be mailed to the manufacturer for dosimetric results, not at all desirable for quality control.

The blood dosimetric methods employed used phantoms made of acrylic, water and clear polystyrene (Figures 1 and 2), easily found materials. Simultaneously, they provide similar mass attenuation coefficients to those of whole blood in the appropriate radiation energy range ($\approx 2.0\%$; $<1.0\%$ and $<2.5\%$, respectively) [120], in accordance with ionizing radiation protocols [121]. Moreover, acrylic and clear polystyrene do not need highly specialized equipment to be machined and are relatively inexpensive. In fact, the proposed dosimetric phantoms can be readily employed in any blood bank quality assurance program.

The isodose curves obtained with FXG, film and TLD dosimeters were similar (Figure 5). The maximum difference in dose observed among the dosimeters was 4%. Despite spatial resolutions of these dosimeters are slightly different, those differences are not relevant in comparison to the minimum and maximum recommended doses. Although the TLD normalized absorbed dose distribution was similar to the other dosimeters, its spatial resolution was lower, because TLD dosimetry is commonly accomplished through individual TLD dosimeters, meaning that discrete readings need to be acquired and later interpolated. Each dosimeter presented reasonable homogeneous regions at the central irradiation area, due to continuous rotation of the canister, and a highest isodose percentage values at the lower mid point of the irradiated volume. Those dose values were presumed to be related both to photon scattering and source alignment. Since the canister top is without a cap, irradiations were not vertically symmetric. However, the energy imparted by the ^{137}Cs photons to the phantom was relatively low (0.662 MeV) and indicates that scattering was not the major contributor to the reported results. Thus, data suggest that the ^{137}Cs source or, at least, the radioactive volume of the source may be misaligned from the vertical center. Nevertheless, even if the available blood irradiator presents a displaced source, the FXG, film and TLD percentage dose distributions indicate that it is still able to irradiate blood at acceptable homogeneity levels.

As recommended by different international guides [51–56], blood is currently irradiated from 25 up to 50 Gy to prevent TA-GVHD. According to our findings, the modified FXG dosimeter provides feasible and linear responses for blood irradiation applications in this absorbed dose range. In addition to dose rate and dose distribution measurements, the proposed FXG dosimetric system can be used by the blood bank staff for a quality assurance method for blood irradiation. In summary, it has been shown that the modified FXG dosimetric system proposed here presents appropriate features for quality assurance control in the clinical environment.

Acknowledgments

Author Contributions

Conceived and designed the experiments: LDL EG PP JB. Performed the experiments: LDL PP EM. Analyzed the data: LDL EG AA. Contributed reagents/materials/analysis tools: LDL DC AA. Wrote the paper: LDL EG AA.

References

1. Kernan NA, Collins NH, Juliano L, Cartagena T, Dupont B, et al. (1986) Cloneable T lymphocytes in T cell-depleted bone marrow transplants correlate with development of graft-versus-host disease. Blood 68: 770–773.
2. Anderson KC, Weinstein HJ (1990) Transfusion-associated graft-versus-host disease. New England Journal of Medicine 323: 315–321.
3. Przepiorka D, LeParc GF, Stovall MA, Werch J, Lichtiger B (1996) Use of irradiated blood components: practice parameter. American Journal of Clinical Pathology 106: 6–11.
4. Ferrara JL, Deeg HJ (1991) Graft-versus-host disease. The New England Journal of Medicine 324: 667–74.
5. Thomaz ED, Herman EC, Greenough WB (1961) Irradiation and marrow infusion in leukemia. Archives of Internal Medicine 107: 829–845.
6. Parkman R, Mosier D, Umansky I, Cochran W, Carpenter CB, et al. (1974) Graft-versus-host disease after intrauterine and exchange transfusions for hemolytic disease of the newborn. The New England Journal of Medicine 290: 359–363.
7. Von Fliendner V, Higby DJ, Kim U (1982) Graft-versus-host reaction following blood transfusion. American Journal of Medicine 72: 951–959.
8. Brubaker DB (1983) Human post transfusion graft-versus-host disease. Vox Sanguinis 45: 401–420.
9. Burns LJ, Westberg MW, Burns CP, Klassen LW, Goeken NE, et al. (1984) Acute graft-versus-host disease resulting from normal donor blood transfusions. Acta Hematologica 71: 270–276.
10. Holland PV (1989) Prevention of transfusion-associated graft-vs-host disease. Archives of Pathology & Laboratory Medicine 113: 285–291.
11. Greenbaum BH (1991) Transfusion-associated garft-versus-host disease: Historical perspectives, incidence, and current use of irradiated blood products. Journal of Clinical Oncology 9: 1889–1902.
12. Jamieson NV, Joysey V, Friend PJ, Marcus R, Ramsbottom S, et al. (1991) Graft-versus-host disease in solid organ transplantation. Transplant International 4: 67–91.
13. Orlin JB, Ellis MH (1997) Transfusion-associated graft-versus-host disease. Current opinion in Hematology 4: 442–448.
14. Kilic SS, Kavurt S, Adim SB (2010) Transfusion-associated graft-versus-host disease in severe combined immunodeficiency. Journal of Investigational Allergology and Clinical Immunology 20: 153–156.
15. Neves JF, Marques A, Valente R, Barata D (2010) Nonlethal, attenuated, transfusion-associated graft-versus-host disease in an immunocompromised child: case report and review of the literature. Transfusion 50: 2484–2488.
16. Arsura EL, Bertelle A, Minkowitz S, Cunningham JNJ, Grob D (1988) Transfusion-associated graft-vs-host disease in a presumed immunocompetent patient. Archives of Internal Medicine 148: 1941–1944.
17. Juji T, Takahashi K, Shibata Y, Ide H, Sakakibara T, et al. (1989) Post-transfusion graft-versus host disease in immunocompetent patients after cardiac surgery in Japan. The New England Journal of Medicine 321: 56.
18. Tahler M, Shamiss A, Orgad S, Huszar M, Nussinovitch N, et al. (1989) The role of blood from hla-homozygous donnors in fatal transfusion-associated graft-versus-host disease after open heart surgery. The New England Journal of Medicine 321: 25–28.
19. Kobayashi H, Kitano K, Kishi E, Hara K, Ishida F, et al. (1993) Transfusion-associated graftversus-host disease in an immunocompetent patient following accidental injury. American Journal of Hematology 43: 51–53.
20. O' Connor NT, Mackintosh P (1992) Transfusion associated graft versus host disease in an immunocompetent patient. Journal of Clinical Pathology 45: 621–622.
21. Ohto H, Yasuda H, Noguchi M, Abe R (1992) Risk of transfusion-associated graft-versus-host disease as a result of directed donations from relatives. Transfusion 32: 691–693.
22. Petz LD, Calhoun P, Yam M (1993) Transfusion-associated graft-versus-host disease in immunocompetent patients: Report of a fatal case associated with transfusion of blood from a seconddegree relative and a survey of predisposing factors. Transfusion 33: 742–750.
23. Van der Mast BJ, Hornstra N, Ruigrok MB, Claas FHJ, van Rood JJ, et al. (1994) Transfusionassociated graft-versus-host disease in immunocompetent patients: a self-protective mechanism. The Lancet 343: 753–757.
24. Ohto H, Anderson KC (1996) Survey of transfusion-associated graft-versus-host disease in immunocompetent recipients. Transfusion Medicine Reviews 10: 31–43.
25. Ahya R, Douglas J, Watso H (1998) Transfusion associated graft versus host disease in an immunocompetent individual following coronary artery bypass grafting. Heart 80: 299–300.
26. Rososhansky S, Badonnel MCH, Hiestand LL, Popovsky MA, Szymanski IO (1999) Transfusionassociated graft-versus-host disease in an immunocompetent patient following cardiac surgery. Vox Sanguinis 76: 59–63.
27. Gorman TE, Julius CJ, Barth RF, Ng A, Kennedy MS, et al. (2000) Transfusion-associated graftvs-host disease. a fatal case caused by blood from an unrelated HLA homozygous donor. American Journal of Clinical Pathology 113: 732–737.

28. Luban NLC, Drothler D, Moroff G, Quinones R (2000) Irradiation of platelet components: Inhibition of lymphocyte proliferation assessed by limiting-dilution analysis. Transfusion 40: 348–352.

29. Aoun E, Shamseddine A, Chehal A, Obeid M, Taher A (2003) Transfusion-associated GVHD: 10 years' experience at the American University of Beirut-Medical Center. Transfusion 43: 1672–1676.

30. Serefhanoglu K, Turan H, Saba T, Ozer I, Tosun E, et al. (2005) Transfusion-associated graftversus-host disease in an immunocompetent individual following cardiac surgery. Journal of the National Medical Association 97: 418–420.

31. Klein HG (2006) Transfusion-associated graft-versus-host disease: less fresh blood and more gray (Gy) for an aging population. Transfusion 46: 878–880.

32. Oto OA, Paydas S, Baslamisli F, Tuncer I, Ergin M, et al. (2006) Transfusion-associated graftversus-host disease. European Journal of Internal Medicine 17: 151–156.

33. Triulzi D, Duquesnoy R, Nichols L, Clark K, Jukic D, et al. (2006) Fatal transfusion-associated graft-versus-host disease in an immunocompetent recipient of a volunteer unit of red cells. Transfusion 46: 885–888.

34. Agbaht K, Altintas ND, Topeli A, Gokoz O, Ozcebe O (2007) Transfusion-associated graft-versushost disease in immunocompetent patients: case series and review of the literature. Transfusion 47: 1405–1411.

35. Patel KK, Patel AK, Ranjan RR, Shah AP (2010) Transfusion associated graft versus host disease following whole blood transfusion from an unrelated donor in an immunocompetent patient. Indian Journal of Hematology and Blood Transfusion 26: 92–95.

36. Crowley JP, Skrabut EM, Valeri CR (1974) Immunocompetent lymphocytes in previously frozen washed red cells. Vox Sanguinis 26: 513–517.

37. Akahoshi M, Takanashi M, Masuda M, Yamashita A, Hasegawa K, et al. (1992) A case of transfusion-associated graft-versus-host disease not prevented by white cell-reduction filters. Transfusion 32: 169–172.

38. Hayashi M, Nishiuchi T, Tamura H, Takeda K (1993) Transfusion-associated graft-versus-host disease caused by leukocyte-filtered stored blood. Anesthesiology 79: 1419–1421.

39. Korngold R (1993) Biology of GVHD. American Journal of Pediatric Hematology Oncology 15: 18–27.

40. Nollet KE, Holland PV (2003) Toward a coalition against transfusion-associated GVHD. Transfusion 43: 1655–1657.

41. Moroff G, Luban NLC (1997) The irradiation of blood and blood components to prevent graftversus-host disease: Technical and guidelines. Transfusion Medicine 11: 15–26.

42. Moroff G, Leitman SF, Luban NLC (1997) Principles of blood irradiation, dose validation, and quality control. Transfusion 37: 1084–1092.

43. Sprent J, Anderson RE, Miller JF (1974) Radiosensitivity of T and B lynphocytes. II effect of irradiation on response of T cells to alloantigens. European Journal of Immunology 4: 204–210.

44. Pelszynski MM, Moroff G, Naomi LC (1994) Effect of irradiation of red blood cell units on Tcell inactivation as assessed by limiting diluiton analysis: Implications for preventing transfusionassociated graft-versus-host disease. Blood 83: 1583–1589.

45. Leitman SF (1993) Dose, dosimetry, and quality improvement of irradiated blood components. Transfusion 33: 447–449.

46. Rosen NR, Weidner JG, Boldt HD, Rosen DS (1993) Prevention of transfusion-associated graftversus-host disease: Selection of an adequate dose of gamma irradiation. Transfusion 33: 125–127.

47. Drobynski W, Thibodeau S, Truitt RL, Baxter-Lowe LA, Gorski J, et al. (1989) Third-partymediated graft rejection and graft-versus-host disease after T-cell-depleted bone marrow transplantation, as demonstrated by hypervariable DNA probes and HLA-DR polymorphism. Blood 74: 2285–2294.

48. Sproul AM, Chalmers EA, Mills KI, Burnett AK, Simpson E (1992) Third party mediated graft rejection despite irradiation of blood products. British Journal of Haematology 80: 251–252.

49. Lowenthal RM, Challis DR, Griffiths AE, Chappell RA, Goulder PJ (1993) Transfusion-associated graft-versus-host disease: Report of an occurrence following the administration of irradiated blood. Transfusion 33: 524–529.

50. Góes EG, Borges JC, Covas DT, Orellana MD, Palma PV, et al. (2006) Quality control of blood irradiation: Determination T cells radiosensitivity to cobalt-60 gamma rays. Transfusion 46: 34–40.

51. FDA (1993) Recommendations regarding license amendments and procedures for gamma irradiation of blood products. Technical report, U.S. Food and Drug Administration. U.S. Department of Health & Human Services (FDA), Bethesda, MD, EUA.

52. AABB (2011) Standards for blood banks and transfusion services. 27th ed. Technical report, American Association of Blood Banks, Bethesda, MD, EUA.

53. BCSH Blood Transfusion Task Force (1996) Guidelines for irradiation of blood and blood components for the prevention of transfusion-associated graft-versus-host disease. Transfusion Medicine 6: 261–271.

54. BCSH (2010) Blood transfusion task force. Technical report, Blood Transfusion Task Force (BCSH). Available: http://www.bcshguidelines.com/documents/irrad_bcsh_072010.pdf.

55. Treleaven J, Gennery A, Marsh J, Norfolk D, Page L, et al. (2010) Guidelines on the use of irradiated blood components prepared by the British Committee for Standards in Haematology blood transfusion task force. British Journal of Haematology 152: 35–51.

56. Council of Europe (2011) Guide to the preparation, use and quality assurance of blood components. recommendation No. R (95) 15. Technical report, Council of Europe, Strasbourg, France.

57. Fricke H, Morse S (1927) The chemical action of roentgen rays on dilute ferrosulphate solutions as a measure of dose. American Journal of Roentgenology, Radium Therapy, and Nuclear Medicine 18: 430–432.

58. Fricke H, Hart EJ (1955) Radiation Dosimetry, New York, NY EUA: Academic Press, volume 2, chapter Chemical Dosimetry. 167–239.

59. Schreiner LJ (2004) Review of Fricke gel dosimeters. Journal of Physics: Conference Series 3: 9–21.

60. American Association of Physicists in Medicine (AAPM) (1983) A protocol for the determination of absorbed dose from high-energy photon and electron beams. Task Group No 21, Radiation Therapy Committee. Medical Physics 10: 741–771.

61. ICRU No 35 (1984) Radiation dosimetry: electron beams with energies between 1 and 50 MeV. Technical report, International Commission on Radiation Units and Measurements (ICRU).

62. Day MJ, Stein G (1950) Chemical effects of ionizng radiation in some gels. Nature 166: 146–147.

63. Andrew HL, Murphy RE, LeBrun EJ (1957) Gel dosimeter for depth dose measurements. Review of Scientific Instruments 28: 329–332.

64. Gore JC, Kang YS, Schulz RJ (1984) Measurement of radiation dose distributions by nuclear magnetic resonance (NMR) imaging. Physics in Medicine and Biology 29: 1189–1197.

65. Olsson LE, Petersson S, Ahlgren L (1989) Ferrous sulphate gels for determination of absorbed dose distributions using MRI technique: Basic studies. Physics in Medicine and Biology 34: 43–52.

66. Day MJ (1990) Radiation dosimetry using nuclear magnetic resonance: an introductory review. Physics in Medcine and Biology 35: 1605–1609.

67. Bero MA, Gilboy WB, Glover PM, El-masri HM (2000) Tissue-equivalent gel for non-invasive spatial radiation dose measurements. Nuclear Instruments and Methods in Physics Research B 166–167: 820–825.

68. Bero MA, Gilboy WB, Glover PM (2000) An optical method for three-dimensional dosimetry. Journal of Radiological Protection 20: 287–294.

69. Gambarini G, Birattari C, Mariani M, Marchesini R, Pirola L, et al. (2004) Study of light transmittance from layers of Fricke-xylenol-orange-gel dosimeters. Nuclear Instruments and Methods in Physics Research B 213: 321–324.

70. Gambarini G, Gomarasca G, Marchesini R, Pecci A, Pirola L, et al. (1999) Three-dimensional determination of absorbed dose by spectrophotometric analysis of ferrous-sulphate agarose gel. Nuclear Instruments and Methods in Physics Research A 422: 643–648.

71. Bero MA, Gilboy WB, Glover PM (2001) Radiochromic gel dosemeter for three-dimensional dosimetry. Radiation Physics and Chemistry 61: 433–435.

72. Cavinato CC, Sakuraba RK, Cruz JC, Campos LL (2010) Spectrophotometric response of the fricke gel dosimeter developed at IPEN for clinical electron beams. Helsinki, Sucia: Proceedings of Third European IRPA Congress.

73. Oliveira LND, Calcina CS, Parada MA, Almeida CED, Almeida AD (2007) Ferrous xylenol gel measurements for 6 and 10 MV photons in small field sizes. Brazilian Journal of Physics 37: 1141–1145.

74. Calcina CSG, de Oliveira LN, de Almeida CE, de Almeida A (2007) Dosimetric parameters for small field sizes using Fricke Xylenol Gel, thermoluminescent and film dosimeters, and an ionization chamber. Physics in Medicine and Biology 52: 1431–1439.

75. Bero M, Zahili M (2009) Radiochromic gel dosimeter (FXG) chemical yield determination for dose measurements standardization. Journal of Physics: Conference Series 164.

76. Hazle JD, Hefner L, Nyerick CE, Wilson L, Boyer AL (1991) Dose-response characteristics of a ferrous-sulphate-doped gelatin system for determining radiation absorbed dose distributions by magnetic resonance imaging (Fe MRI). Physics in Medcine and Biology 36: 1117–1125.

77. Gambarini G, Arrigoni S, Cantone MC, Molho N, Facchielli L, et al. (1994) Dose-response curve slope improvement and result reproducibility of ferrous-sulphate-doped gels analysed by NMR imaging. Physics in Medcine and Biology 39: 703–717.

78. Kron T, Jonas D, Pope JM (1997) Fast T1 imaging for NMR dosimetry and di_usion measurement in dosimetry gel samples. Magnetic Resonance Imaging 15: 211–221.

79. Bero MA, Kharita MH (2004) Effects of ambient temperature on the FXG radiochromic gels used for 3-D dosimetry. Journal of Physics: Conference Series 3.

80. Vergote K, Deene YD, Duthoy W, Gersem WD, Neve WD, et al. (2004) Validation and application of polymer gel dosimetry for the dose verification of an intensity-modulated arc therapy (IMAT) treatment. Physics in Medcine and Biology 49: 287–305.

81. Tarte BJ, Jardine PA, van Doorn T, Nitschke KN, Poulsen MG (1997) Development of a CCD array imaging system for measurement of dose distributions in doped agarose gels. Medical Physics 24: 1521–1525.

82. Kelly RG, Jordan KJ, battista JJ (1998) Optical CT reconstruction of 3D dose distributions using the ferrous-benzoic-xylenol (FBX) gel dosimeter. Medical Physics 25: 1741–1750.

83. Jenneson P, Bero MA, Gilboy WB, Doran SJ, Morton EJ (1999) Three-dimensional optical tomography of dose distribution using radiation sensitive transparent gels. In: Nuclear Science Symposium. Conference Record. IEEE. volume 1, 538–540.

84. Wolodzko JG, Marsden C, Appleby A (1999) CCD imaging for optical tomography of gel radiation dosimeters. Medical Physics 26: 2508–2513.

85. Doran SJ, Koerkamp KK, Bero MA, Jenneson P, Morton EJ, et al. (2001) A CCD-based optical CT scanner for high resolution 3D imaging of radiaiton distributions: equipment specifications, optical simulations and preliminary results. Physics in Medcine and Biology 46: 3191–3214.

86. Sato R, de Almeida A, Moreira MV (2009) 137Cs source dose distribution using the Fricke Xylenol Gel dosimetry. Nuclear Instruments and Methods in Physics Research B 267: 842–845.

87. Czelusniak C, Del Lama LS, Moreira MV, Almeida AD (2010) Evaluation of the breast absorbed dose distribution using the Fricke Xylenol Gel. Journal of Physics: Conference Series 250.

88. Alva M, Sampaio FGA, Moreira MV, Petchevist P, Almeida AD (2010) Absorbed dose distribution visualization for superficial treatments through the Fricke Xylenol Gel dosimeter (FXG). Journal of Physics: Conference Series 250.

89. Sampaio FGA, Del Lama LS, Moreira MV, de Almeida A (2011) Gap application results for adjacent electron beams treatment. Nuclear Instruments and Methods in Physics Research B 269: 3141–3144.

90. Sampaio FGA, Del Lama LS, Sato R, de Oliveira DMM, Czelusniak C, et al. (2013) Quality assurance of a two-dimensional CCD detector system applied in dosimetry. IEEE Transactions on Nuclear Science 60: 810–816.

91. Caldeira AMF, Neto AM, Bento AC, Baesso ML, Silva MA, et al. (2007) Behavior of oxidation in the radiochromic gel dosimeter through photoacoustic technique measurements. Applied Radiaton and Isotopes 65: 605–609.

92. Caldeira AMF, de Almeida A, Neto AM, Baesso ML, Bento AC, et al. (2007) Fricke Xylenol Gel characterization using photoacoustic technique. Nuclear Instruments and Methods in Physics Research A 582: 484–488.

93. IAEA (2000) Absorbed dose determination in external beam radiotherapy: An international code of practice for dosimetry based on standars of absorbed dose to water. technical reports series 398. Technical report, International Atomic Energy Agency (IAEA), Viena, Áustria.

94. Masterson ME, Febo R (1992) Pretransfusion blood irradiation: Clinical rationale and dosimetric considerations. Medical Physics 19: 649–657.

95. Aukett RJ (1991) A technique for the local measurement of air kerma rate from small caesium-137 sources. British Journal of Radiology 64: 918–922.

96. Joint Committee for Guides in Metrology (2008) Evaluation of measurement data – Guide to the expression of uncertainty in measurement. Technical report.

97. ISO/ASTM (2005) 51707. Estimating uncertainties in dosimetry for radiation processing. Technical report.

98. ICRU No 50 (1993) Prescribing, recording and reporting photon beam therapy. Technical report, International Commission on Radiation Units and Measurements (ICRU), Bethesda, MD, EUA.

99. Almond PR, Biggs PJ, Coursey BM, Hanson WF, Huq MS, et al. (1999) AAPMs TG-51 protocol for clinical reference dosimetry of high-energy photon and electron beams. Medical Physics 26: 1847–1870.

100. Johns HE, Cunningham JR (1983) The Physics of Radiology. Springfield, IL, EUA: Charles C. Thomas, 4th edition.

101. Attix FH (1986) Introduction to Radiological Physics and Radiation Dosimetry. New York, NY, EUA: John Wiley & Sons, 2nd edition.

102. Podgorsak EB (2005) Radiation Oncology Physics: A handbook for teachers and students. Viena, ustria: International Atomic Energy Agency.

103. Khan FM (2009) The Physics of Radiation Therapy. Philadelphia, PA, EUA: Lippincott Williams & Wilkins, 4th edition.

104. Ibbott GS (2004) Applications of gel dosimetry. Journal of Physics: Conference Series 3: 58–77.

105. Taylor ML, Franich RD, Trapp JV, Johnston PN (2008) The effective atomic number of dosimetric gels. Australasian Physical & Engineering Sciences In Medicine 31: 131–138.

106. Kumar TK, Reddy KV (1997) Effective atomic numbers for materials of dosimetric interest. Radiation Physics and Chemistry 50: 545–553.

107. Cutnell JD, Johnson KW (1998) Physics. Wiley, 4th edition.

108. Law J (1970) Variation of response of the FeSO4 dosemeter with temperature of the solution during irradiation. Physics in Medcine and Biology 15: 741–742.

109. Mattsson LO, Johansson KA, Svensson H (1982) Ferrous sulphate dosemeter for control of ionization chamber dosimetry of electron and 60Co gamma beams. Acta Oncologica 21: 139–144.

110. Shortt KR (1989) The temperature dependence of $G(Fe^{+3})$ for the Fricke dosemeter. Physics in Medcine and Biology 34: 1923–1926.

111. Graw RG, Whang-Peng J, Krüger G, Buckner CD, Leventhal BG, et al. (1970) Complication of bone-marrow transplantation graft-versus-host disease resulting from chronic-myelogenousleukmia leucocyte transfusions. The Lancet 296: 338–341.

112. Bogner L, Hartl P, Scherer J, Treutwein M, Herbst M (1998) Dosimetry of blood irradiator. Strahlentherapie und Onkologie 174: 431–436.

113. Kronholz HL, Moustakis C, Wullenweber J (1998) Blood irradiators - technique, dosimetry and suggestions to quality assurance. Infusion Therapy and Transfusion Medicine 25: 56–61.

114. Butson MJ, Yu PKN, Cheung T, Carolan MG, Quach KY, et al. (1999) Dosimetry of blood irradiaton with radiochromic film. Transfusion Medicine 9: 205–208.

115. Hillyer CD, Hall JM, Lackey DA, Wazer DE (1993) Developmento of colorimetric dosimeter for quality control of blood units and irradiators. Transfusion 33: 898–901.

116. McLaughlin WL, ÒHara KPJ (1996) The importance of reference standard and routine absorbeddose measurements in blood irradiation. Transfusion, Administrative Section, 67s–89s, abstract A61 36.

117. Feinstein C, Winkler E, Saravi M (2000) ESR/alanine gamma dosimetry in the 10–30 Gy range. Applied Radiation and Isotopes 52: 1195–1196.

118. Chen F, Covas DT, Baffa O (2001) Dosimetry of blood irradiation using an alanine/ESR dosimeter. Applied Radiation and Isotopes 55: 13–16.

119. Cheung T, Butson M, Yu PKN (2001) Validation of blood product irradiation doses. Physics in Medcine and Biology 46: N241–N244.

120. NIST (2010) X-ray mass attenuation coefficients. URL http://physics.nist.gov/PhysRefData/XrayMassCoef/tab4.html.

121. ICRU No 44 (1989) Tissue substitutes in radiation dosimetry and measurement (report 44). Technical report, International Commission on Radiation Units and Measurements (ICRU), Bethesda, MD, EUA.